ORIGINAL

Jordan F. Clark · Ira Leifer · Libe Washburn
Bruce P. Luyendyk

Compositional changes in natural gas bubble plumes: observations from the Coal Oil Point marine hydrocarbon seep field

Abstract Detailed measurements of bubble composition, dissolved gas concentrations, and plume dynamics were conducted during a 9-month period at a very intense, shallow (22-m water depth) marine hydrocarbon seep in the Santa Barbara Channel, California. Methane, carbon dioxide, and heavier hydrocarbons were lost from rising seep bubbles, while nitrogen and oxygen were gained. Within the rising seawater bubble plume, dissolved methane concentrations were more than 4 orders of magnitude greater than atmospheric equilibrium concentrations. Strong upwelling flows were observed and bubble-rise times were ~40 s, demonstrating the rapid exchange of gases within the bubble plume.

Introduction

Marine sediments contain some of the largest reservoirs of methane in the world. These reservoirs include shallow gas hydrates that have both biogenic and thermogenic sources (Kvenvolden 1993, 1995; Sassen et al. 1999), and deeper hydrocarbon accumulations. Leakage from these reservoirs is potentially a significant source of atmospheric methane, one of the most important greenhouse gases. Additionally, marine seeps are significant sources of dissolved hydrocarbons and oil in coastal waters (e.g., Clark et al. 2000; MacDonald et al. 2000; NCR 2002).

J. F. Clark (✉) · B. P. Luyendyk
Department of Geological Sciences,
University of California, Santa Barbara, CA 93106, USA
E-mail: jfclark@geol.ucsb.edu
Tel.: +1-805-8937837
Fax: +1-805-8932314

I. Leifer
Chemical Engineering Department,
University of California, Santa Barbara, CA 93106, USA

L. Washburn
Department of Geography,
University of California, Santa Barbara, CA 93106, USA

Estimates of the magnitude of the global methane flux from marine sediments to the atmosphere are based upon statistical analysis of very limited field measurements of seepage rates (e.g., Hovland et al. 1993; Judd et al. 1997; Hornafius et al. 1999; Kvenvolden et al. 2001; Judd et al. 2002). Because most measurements of seepage rates have been made near the seafloor, these estimates are primarily for leakage from sediments into the ocean (see Judd et al. 2002 for a review). Methane released at the seafloor forms bubble plumes that travel through the water column before entering the atmosphere. Hence, before the atmospheric flux can be estimated, oceanic processes governing methane bubble dissolution must be considered.

The extent to which methane and other gases exchange between bubbles and seawater depends upon the immediate seep and bubble plume environment (Leifer et al. 2000; Leifer and Clark 2002; Leifer and Patro 2002). Models that consider only gas transfer out of single rising bubbles within a stagnant fluid (e.g., Cline and Holmes 1977) are simplifications that overestimate the amount of methane that dissolves because bubble plume processes and ambient conditions are not considered. While some of these processes have been examined in the laboratory (e.g., McDougal 1978; Leifer and Patro 2002), very few studies of marine bubble plumes have been conducted. To address this deficiency, a field program was initiated at a very active, shallow (22-m water depth) hydrocarbon seep found off the coast of California in the Santa Barbara Channel. During this program, water and gas samples, which were collected between the sediments and air–water interface, were combined with physical measurements of the bubble plume environment.

Study site

The northern margin of the Santa Barbara Channel is one of the most active areas of natural marine hydrocarbon

seepage in the world (Hovland et al. 1993). Within the channel, the most concentrated area of seepage is found a few kilometers offshore from Coal Oil Point above the South Ellwood and Coal Oil Point anticlines in 20–70 m deep water (e.g., Fischer 1978; Fig. 1). Trapped within the South Ellwood anticline is a significant hydrocarbon reservoir that has been under production at Platform Holly since the late 1960s. Recent sonar surveys of the seep field indicate that about 1.5×10^5 m^3 day^{-1} of seep gas is emitted to the atmosphere from about 3 km^2 of seafloor (Hornafius et al. 1999). Seep bubbles collected at the surface are about 60% methane (CH$_4$), 30% air (N$_2$+O$_2$), and 10% higher hydrocarbons by volume (Leifer et al. 2000). The CH$_4$ flux from this field is about 35 mol s^{-1} (0.001 Tg year^{-1}). Surveys of the dissolved methane plume immediately downcurrent from the seeps indicate that approximately half of the methane released at the seafloor dissolves during the bubbles' transit through the water column (Clark et al. 2000).

During this study, detail observations were made at Shane Seep (34°24.369′N, 119°53.418′W), which lies inshore of the main field at a water depth of 22 m (Fig. 1). Because of its shallow depth, observations and measurements of the seafloor vents and bubble plume can be conducted easily by SCUBA divers. The seafloor expression of Shane Seep is distributed over an area of about 100 m^2 and consisted of numerous (order of 10^3) small vents surrounding two large tar and mud volcanoes. Each volcano had a diameter of about 3 m and rose about 1 m above the surrounding seafloor. Bacterial mats cover most of the seafloor in the seep area. Gas emitted from these vents rises as bubbles through the water column to the atmosphere. At the surface, bubbles were primarily found in an area of 100–400 m^2. Within this large area, most bubbles appear concentrated within two separate plumes, each having a radius of about 1.5 m. There is a significant radial flow of water (divergence) from the center of each of these plumes.

Visual observations of the seep intensity indicate that the flux varies on the timescale of seconds to tens of minutes. Intense bursts with lifetimes on the order of one minute are commonly observed. The contribution of these bursts to the total flux has not been investigated. In addition to these relatively small bursts, much larger eruptions occur with a frequency of weeks to months. Some of these very large eruptions have caused significant changes to the seafloor morphology.

Bubble dynamics

As seep bubbles rise from the seafloor, they exchange gases with the surrounding water. This exchange occurs in a modified environment that consists of three distinct parts: the rising bubbles, surrounding plume water, and ambient ocean (e.g., McDougal 1978). Bubbles dissolve and shrink as CH$_4$ and heavier hydrocarbons outflow, and expand as dissolved air, primarily N$_2$ and O$_2$, inflows. Furthermore, bubble expansion occurs due to the decreasing hydrostatic pressure. The gas flux across the bubble–water interface, F, is:

$$F = \frac{dn}{dt} = k_B 4\pi r^2 \left(C_{aq} - \frac{P_B}{H} \right)$$

where k_B is the bubble gas transfer rate for a specific gas, r is the bubble equivalent radius (i.e., if the bubble were a sphere), H is the Henry's Law coefficient, C_{aq} is the aqueous concentration, and P_B is the partial pressure of bubble gases. P_B is the product of the gas mole fraction and the sum of the hydrostatic and surface tension (P_{ST}) pressures. P_{ST} is negligible for all but the smallest bubbles ($P_{ST} = 0.1$ atm for an $r = 15$ μm bubble).

The gas flux is driven by the concentration gradient across the interface ($C_{aq} - P_B/H$). Gas outflow occurs when $C_{aq} < P_B/H$, while inflow occurs when $C_{aq} > P_B/H$. If the aqueous concentration of CH$_4$ and other seep gases within the bubble plume water is significantly

Fig. 1 Map of the Coal Oil Point seep field. The locations of the major seafloor features and the August 1996 seepage distribution are from Quigley et al. (1999)
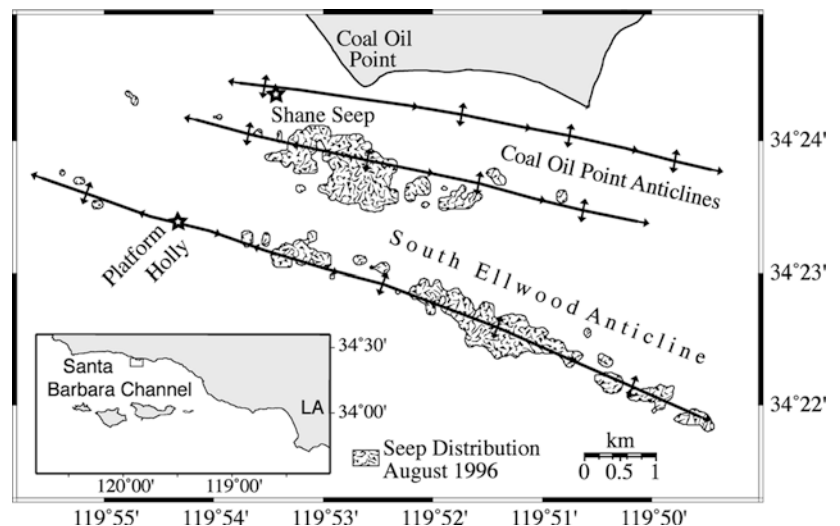
elevated due to bubble dissolution, the flux of these gases from the bubbles to the seawater is decreased. When this decrease in dissolution occurs, more gas is transported and released into the atmosphere (i.e., a smaller fraction dissolves). If the dissolved O_2 and N_2 concentrations in the bubble plume water are significantly depleted, inflow of air will be reduced.

In addition to the concentration gradient, the gas flux also depends upon r, the gas diffusivity (D), bubble surface cleanliness (e.g., oiliness), and small-scale ($\sim r$) turbulence (Leifer and Patro 2002). The former two parameters are important because the bubble gas transfer rate, k_B, is a function of r and D (i.e., larger bubbles are significantly more efficient at gas transfer).

The total gas entering the water column depends upon the integrated flux over the bubble's lifetime. Thus, the rise velocity, which is a function of both the bubble buoyancy (radius) and possible upwelling flows generated by the bubble plume, is critical. Large bubble plumes that generate upwelling flows significantly decrease the transit time from the seafloor to the surface, and thus increase the flux of seep gas to the atmosphere.

Materials and methods

The bubbling gas flux just below the water surface (~ 2.5 m depth) at Shane Seep was measured using an instrumented spar buoy described by Washburn et al. (2001). The instrument, called the Flux Buoy, uses an inverted funnel (~ 0.5 m diameter) to capture gas directly and measure its flux every second. The instrument was gently towed over Shane Seep behind a small boat. Shaded and closed dots in Fig. 2A show the measurement locations. The total flux was estimated by averaging all flux measurements in a reference area and then multiplying this reference area by the average flux. The reference area was determined by finding the mean position of flux measurements above a threshold (5 m^3 m^{-2} day^{-1}), and then enclosing the high flux region within a square area centered on this position. A square, subjectively chosen to be 20 m on a side, was found to enclose the region of highest flux (cf. square in Fig. 2A).

Dissolved gas and bubble samples were collected at Shane Seep by SCUBA divers on three occasions in 2001—2 February, 22 August, and 10 October. Each time, samples were collected 1 m above the tar volcanoes (~ 20 m), at mid-depth (~ 10 m) and 1 m below the surface (~ 1 m). At each depth, seep bubbles were trapped in a plastic bag and sampled with 50-ml glass syringes. Following the gas sampling, bubble-free water samples of the plume were collected in either 50-ml or 100-ml glass syringes by slowly filling the syringes with the tip pointed up while the divers leaned backwards. By holding the syringes in this position, the driver's body diverted the rising bubbles away from the syringe tip, ensuring that no bubbles were collected. All of the
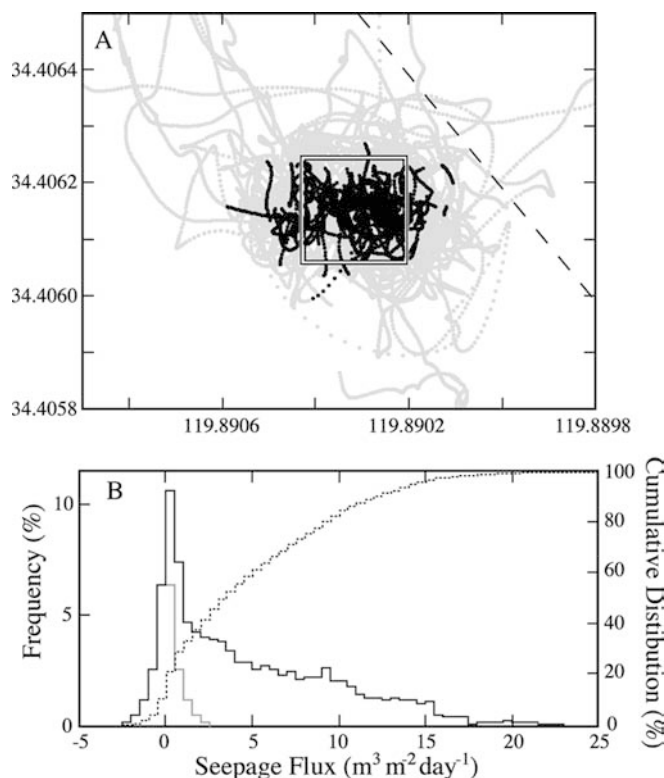

Fig. 2 A Spatial distribution of flux observations obtained from the Flux Buoy on 15 and 23 August 2002 (*shaded* and *closed dots*) at Shane Seep. Locations with flux exceeding 5 m^3 m^{-2} day^{-1} are indicated by *closed dots*. The *square* indicates the 400-m^2 reference area used for estimating total flux. The 20-m isobath is indicated by a *dashed line* that slopes up to the *left*. **B** Histogram (*darkly shaded solid line*) and cumulative distribution (*dotted line*) for flux values in the reference area. The *lightly shaded solid line* is the reflection of the negative flux values on the histogram

syringes were submerged in cold seawater until they were processed in the laboratory.

In the laboratory, the gas samples were transferred directly to pre-evacuated 20-ml septa tubes in an argon (Ar)-rich atmosphere that was created by continuously flushing a large plastic box with high-purity Ar. The dissolved gas concentrations of water samples were determined using the headspace method. The syringes were moderately shaken for 10 min to equilibrate the water with the headspace. The headspace gas was then transferred into septa tubes in the Ar-rich atmosphere. Mole fractions of fixed gases (N_2, O_2, CO_2, CH_4, and H_2) and n-alkanes (CH_4, C_2H_6, C_3H_8, C_4H_{10}, C_5H_{12}) were determined using standard thermal conductivity detector (TCD) and flame ionization detector (FID) gas chromatographic techniques by Inland Empire Analytical (Norco, CA). Ar carrier gas was used during the analysis of air so that the O_2 mole fraction could be determined without interference. The analytical uncertainties of the gas analyses were $\pm 2\%$. Septa tubes blanks, which were determined by filling with high-purity Ar, were free of air and hydrocarbons.

Bubbles at Shane Seep were imaged with a bubble measurement system described in Leifer and MacDonald

(2003). Key features include a remotely controlled underwater video camera with shutter speed and iris control, backlit translucent screen, and bubble blocking plates that minimize the measurement volume so that all bubbles are in focus and at a known distance from the camera. Shutter speed was high enough (typically 1/4,000 s or faster) so that bubble images did not streak. Backlit bubbles appear as dark rings with bright centers, allowing computer identification and discrimination from non-gas-filled objects (i.e., sediment, marine fauna, etc.). Video images were digitized at 60 fields per second and bubbles were tracked across the field of view to determine rise speed. The mean radius and vertical velocity were calculated from the measurement sequence for each bubble, and the process was repeated for all bubbles in each video sequence.

Results

Observations at Shane Seep on 15 and 23 August 2002 using the Flux Buoy showed that high fluxes commonly occur at this seep. About 40% of the 6,154 flux measurements within the 20-m square reference area exceeded 5 m^3 m^{-2} day^{-1} (closed dots, Fig. 2A), as shown by the histogram and cumulative distribution in Fig. 2B. The highest values at Shane Seep exceeded 20 m^3 m^{-2} day^{-1}, making them among the largest observed to date in the entire Coal Oil Point seep field. The histogram of flux (Fig. 2B) shows some negative values that are artifacts (noise) from the vertical motion of the seep buoy due to wave action and towing (Washburn et al. 2001). If these negative values are reflected across the y-axis (lightly shaded solid line, Fig. 2B), they show that most observed flux values greatly exceeded noise levels. The total gas flux at Shane Seep was estimated to be about 1,900 m^3 day^{-1}. Thus, this seep contributes approximately 2% of the entire field's flux.

The depth pattern of the bubble gas composition was observed to be very uniform over the nine months of observations (Table 1, Fig. 3). The standard deviations of the gas mole fractions were less than 3%, approximately the same as the analytical uncertainty. The bubbles 1 m above the tar volcanoes were composed primarily of CH_4 (83%), CO_2 (12%), and NMHC (non-methane hydrocarbons, 2.9%); components of air (N_2 and O_2) contributed less than 2% of the total volume. At shallower depths, the CO_2 mole fraction decreased to the analytical detection limit whereas the air fraction increased (Fig. 3). At the surface, bubbles were composed

Table 1 Mean bubble composition, bubble gas ratios, and mean dissolved CH_4 concentrations within the Shane Seep bubble plume

Depth (m)	Date	n^a	CH_4 (%)	N_2 (%)	O_2 (%)	CO_2 (%)	NMHC (%)	N_2/CH_4	N_2/O_2	n^b	CH_4 (μmol/l)
1	2 February	4	79.4	13.8	4.5	>0.1	2.2	0.175	3.11	-	-
1	22 August	6	76.7	14.4	6.0	>0.1	-	0.188	2.41	2	42.6
1	10 October	2	79.5	12.6	5.0	>0.1	2.8	0.158	2.53	2	56.9
10	2 February	2	90.8	4.9	1.8	0.2	2.4	0.054	2.78	2	20.6
10	22 August	2	84.4	8.1	3.0	0.1	-	0.096	2.67	3	59.6
10	10 October	2	86.4	7.5	2.8	>0.1	3.2	0.087	2.65	2	48.6
20	2 February	1	84.2	2.5	0.3	10.6	2.3	0.029	7.54	1	36.6
20	22 August	4	81.9	1.4	0.2	13.4	-	0.017	5.86	3	42.3
20	10 October	4	84.0	1.5	0.3	11.2	3.0	0.031	5.14	3	65.7

[a]Number of bubble samples analyzed
[b]Number of water samples analyzed

Fig. 3 Depth dependence of the major components of the gas bubbles above Shane Seep, showing the mean and standard deviation of all samples collected on the three different sampling trips
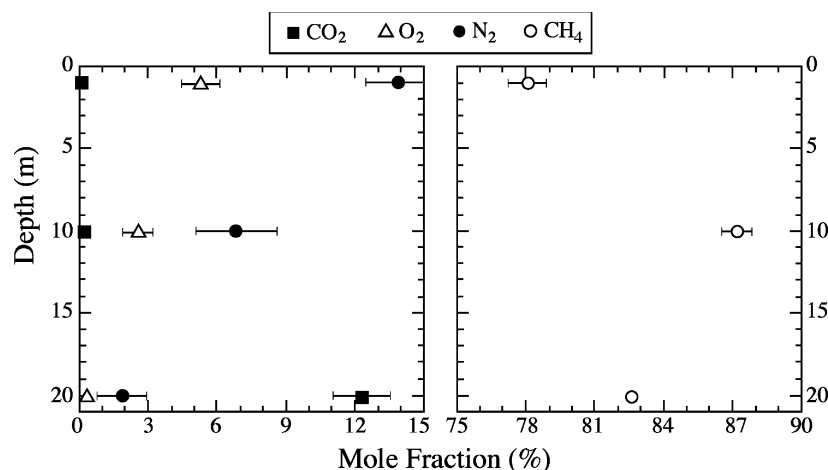
of CH_4 (78%), N_2 (14%), O_2 (5.3%), and NMHC (2.4%). The mole fraction of CH_4 and NMHC reached a maximum at mid-depths due to the more rapid loss of CO_2 (Table 1, Fig. 3) relative to the inflow of N_2 and O_2. As is apparent in the N_2/CH_4 ratio, the amount of CH_4 decreased continuously relative to N_2 as the bubbles rose through the water column (Table 1).

At mid-depth and the surface, the bubble N_2/O_2 ratio (2.4 to 3.1; see Table 1) was less than the atmospheric ratio (3.7) and greater than the atmospheric equilibrium ratio in seawater at 10 °C (1.8). The ratios were equivalent to the expected ratio of 10 °C seawater in which 25–42% of the O_2 had been consumed. At the seafloor, the ratio (>5) is greater than the atmosphere, as would be expected from either a sedimentary or crustal source. The non-zero O_2 concentration in the seafloor samples suggests that a small amount of exchange with seawater had occurred prior to sampling. The change in the N_2/O_2 ratio to values typical of coastal ocean water, combined with the increase in mole fraction of these two gases, clearly demonstrates that rising seep bubbles strip gas from the water column.

Aqueous CH_4 concentrations within the plume water showed greater variability than the bubble gas composition. The concentration ranged between 30 and 125 μM and did not vary systematically with either position (center vs. edge of the bubble plume) or depth. The observed concentrations were more than 4 orders of magnitude above atmospheric equilibrium concentrations, and $<10\%$ of equilibrium concentrations with the seep bubbles. The mean degree of saturation of the plume water at each sampling depth increased from about 1.5% near the seafloor to about 5.5% at the water surface. This change was primarily due to the decrease in the hydrostatic pressure between the seafloor and surface. The observed surface concentrations at Shane Seep were about an order of magnitude less than those observed at deeper seeps within the Coal Oil Point seep field (Leifer et al. 2000).

The duration of exchange between the bubbles and plume water is defined by the bubble's rise time from the seafloor to the surface. The rate of rise is a function of both the upwelling flow and the bubble's buoyancy. Upwelling flows were determined directly from the transit time to the surface of dye (Fluorescein) released into the bubble plume above the tar volcano crater. Dye release experiments were conducted on two occasions and yielded similar results. Released dye was first observed at the surface after about 50 s. The color of the dye patch on the surface continued to darken for the next one to two minutes as a result of both non-instantaneous release and spatial variations in the upwelling flows within the plume. The maximum upwelling velocity, which defines the flow in the plume axis (McDougal 1978), was determined with the initial arrival of the dye at the surface and was found to be about 40 cm s^{-1}.

Direct observations of bubble-rise velocities near the surface and seafloor using the video bubble measurement system confirmed the presence of an upwelling flow. The size-dependent bubble-rise velocity averaged over all bubbles in each size class near the water surface (about 0.3-m depth) is shown in Fig. 4, along with the clean and dirty bubble parameterized rise velocities (Clift et al. 1978). Although bubbles from Shane Seep are oily (at the surface they leave a sheen), the larger bubbles rise faster than even the clean-bubble parameterization. This difference, about 15 cm^{-1}, is an estimate of the upwelling velocity. At the seafloor, upwelling velocities were found to be significantly different between the small (about 15 cm s^{-1}) and large (about 40 cm s^{-1}) vents, and slightly higher than at the surface. The combination of the effects of bubble buoyancy and upwelling flow indicates that the bubble-rise time from the seafloor vents to the surface is about 40 s. Hence, the exchange of gases between the bubbles and plume water occurs very rapidly.

Discussion and conclusions

The field study at Shane Seep illustrates the important chemical and physical processes that occur in the modified environment of large bubble plumes. Despite the very short travel time of bubbles from the seafloor to the surface ($\sim$40 s), a significant amount of gas exchange between the bubbles and plume water occurs, creating distinctly different seafloor and surface gas compositions. Furthermore, enough CH_4 was lost from the bubbles to increase the dissolved CH_4 concentration within the plume by more than 4 orders of magnitude above atmospheric equilibrium values. However, there was insufficient time to bring the plume water into equilibrium with the bubbles (i.e., [CH_4] $<10\%$ saturation).

Leifer et al. (2000) reported that, at the surface of the ocean, concentrations of CH_4 within the bubble plumes of deeper, large Coal Oil Point seeps (50 to 70 m) were slightly supersaturated. This observation demonstrates
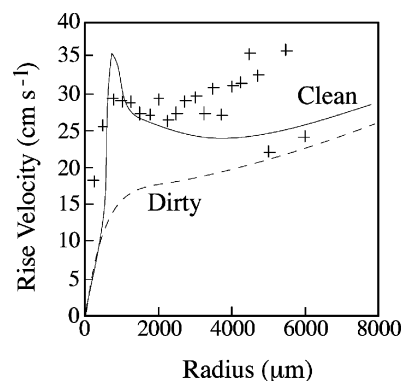

Fig. 4 Mean rise velocity of discrete bubble size classes near the surface of Shane Seep (30-cm depth). The *solid* and *dashed* lines represent laboratory-determined rise velocities in stagnant water respectively for clean and dirty bubbles derived from Clift et al. (1978)

that, given enough time, large bubble plumes can saturate the plume water with CH_4 and, thus, the loss of this gas from the bubbles will cease. Once saturated, the CH_4 remains in the seep bubbles and is transported through the water column directly to the atmosphere. The depth of CH_4 saturation in the Coal Oil Point seep field is relatively shallow, between 20 and 50 m.

The Coal Oil Point seeps studied during this investigation and by Leifer et al. (2000) are some of the largest in the world. It is likely that the processes observed in these seeps occur on a reduced scale in much smaller seeps. Bubbles from seeps that are unable to saturate the plume water continue to lose CH_4 throughout the water column. Given enough time (sufficient depth), the bubbles may even dissolve completely (e.g., Leifer and Judd 2002).

It is apparent that the size of a seep is critical for determining the fraction of CH_4 released at the seafloor that is emitted to the atmosphere. A greater fraction of the gas released at the seafloor from small seeps dissolves into the water column than from large seeps. Thus, small seeps are more efficient at transferring CH_4 into the water column, and less efficient at transferring CH_4 to the atmosphere than are large seeps. As a result, the atmospheric CH_4 source from marine sediments is probably dominated by the flux from large seeps. Global CH_4 source estimates need to take this fact into consideration.

The observations of bubble plumes made at the Coal Oil Point seep field provide valuable insights into the behavior of large seeps. These insights can also be applied to larger seafloor gas releases, such as those expected from catastrophic events. It is likely that during these events, the plume water will become saturated with CH_4 and large upwelling flows will develop. Once the transfer of CH_4 out of the bubbles ceases (due to saturation), bubbles should rise to the sea surface regardless of ocean depth. Thus, these processes create the potential for very efficient transfer of seep gases from the seafloor to the atmosphere, even if the release depth is significantly greater than found in the Coal Oil Point seep field.

The upwelling flows associated with bubble plumes will deposit water saturated with CH_4 at the sea surface. The amount of CH_4 deposited by this flow to the surface is significantly greater than the amount that would be added only through bubble dissolution. Presumably, the majority of the dissolved CH_4 will be lost rapidly either to in-situ oxidization or to the atmosphere via air–sea gas exchange. However, because these processes are not instantaneous, the upwelled, CH_4-rich water will flood the mixed layer, creating an inverted CH_4 concentration profile near the surface (i.e., the mixed layer concentrations will be greater than the deep thermocline and, probably, the mid-water column concentrations). This process may help to explain the very large negative $\delta^{13}C$ deviations observed in some paleoclimate records of planktonic Foraminifera, such as those found in the Santa Barbara Channel (Kennett et al. 2000). These negative shifts have been interpreted to result from massive releases of methane from the seafloor. Because of the large upwelling flows associated with bubble plumes, these $\delta^{13}C$ deviations in planktonic Foraminifera can be produced without significantly increasing the CH_4 concentration throughout the entire water column.

References

Clark JF, Washburn L, Hornafius JS, Luyendyk BP (2000) Dissolved hydrocarbon flux from natural marine seeps to the southern California Bight. J Geophys Res 105:11,509–11,522

Clift R, Grace JR, Weber ME (1978) Bubbles, drops, and particles. Academic Press, New York

Cline JD, Holmes ML (1977) Submarine seepage of natural gas in Norton Sound, Alaska. Science 198:1149–1153

Fischer PJ (1978) Oil and tar seeps, Santa Barbara basin, California. In: California offshore gas, oil, and tar seeps. California State Lands Commission, Sacramento, California, pp 1–62

Hornafius JS, Quigley D, Luyendyk BP (1999) The world's most spectacular marine hydrocarbon seeps (Coal Oil Point, Santa Barbara Channel, California): quantification of emissions. J Geophys Res 104:20,703–20,711

Hovland M, Judd AG, Burke RA Jr (1993) The global flux of methane from shallow submarine sediments. Chemosphere 26:559–578

Judd AG, Davies G, Wilson J, Holmes R, Baron G, Bryden I (1997) Contributions to atmospheric methane by natural seepages on the U.K. continental shelf. Mar Geol 140:427–455

Judd AG, Hovland M, Dimitrov LI, Garcia-Gil S, Jukes V (2002) The geological methane budget at continental margins and its influence on climate change. Geofluids 2:109–126

Kennett JP, Cannariato KG, Hendy IL, Behl RJ (2000) Carbon isotopic evidence for methane hydrate instability during quaternary interstadials. Science 288:128–133

Kvenvolden KA (1993) Gas hydrates—geological perspective and global change. Rev Geophys 31:173–187

Kvenvolden KA (1995) A review of the geochemistry of methane in natural gas hydrate. Org Geochem 23:997–1008

Kvenvolden KA, Lorenson TD, Reeburgh WS (2001) Attention turns to naturally occurring methane seeps. EOS 82:457

Leifer I, Clark JF (2002) Modeling trace gases in hydrocarbon seep bubbles: application to marine hydrocarbon seeps in the Santa Barbara Channel. Russian Geol Geophys 47:572–579

Leifer I, Judd AJ (2002) Oceanic methane layers: the hydrocarbon seep bubble deposition hypothesis. Terra Nova 16:471–425

Leifer I, MacDonald IR (2003) Dynamics of the gas flux from shallow gas hydrate deposits: interaction between oily hydrate bubbles and the oceanic environment. Earth Planet Sci Lett 210:411–424

Leifer I, Patro RK (2002) The bubble mechanism for methane transport from the shallow sea bed to the surface: a review and sensitivity study. Cont Shelf Res 22:2409–2428

Leifer I, Clark JF, Chen RF (2000) Modifications of the local environment by natural marine hydrocarbon seeps. Geophys Res Lett 27:3711–3714

MacDonald IR, Buthman DB, Sager WW, Peccini MB, Guinasso NL (2000) Pulsed oil discharge from a mud volcano. Geology 28:907–910

McDougal TJ (1978) Bubble plumes in stratified environments. J Fluid Mech 4:655–672

NRC (2002) Oil in the sea III: inputs, fates, and effects. National Research Council, National Academy Press

Quigley DC, Hornafius JS, Luyendyk BP, Francis RD, Clark J, Washburn L (1999) Decrease in natural marine hydrocarbon seepage near Coal Oil Point, California associated with offshore oil production. Geology 27:1047–1050

Sassen R, Joye S, Sweet ST, DeFreitas DA, Milkov AV, Mac-Donald IR (1999) Thermogenic gas hydrates and hydrocarbon gases in complex chemosynthetic communities, Gulf of Mexico continental slope. Org Geochem 30:485–497

Washburn L, Johnson CG, Gotschalk CC, Egland ET (2001) A gas-capture buoy for measuring bubbling gas flux in oceans and lakes. J Atmos Ocean Technol 18:1411–1420